



Observation of nontrivial spin-orbit torque in single-layer ferromagnetic metalsQingwei Fu, Like Liang , Wenqiang Wang, Liupeng Yang, Kaiyuan Zhou, Zishuang Li, Chunjie Yan, Liyuan Li, Haotian Li, and Ronghua Liu ^{*}*National Laboratory of Solid State Microstructures, School of Physics and Collaborative Innovation Center of Advanced Microstructures, Nanjing University, Nanjing 210093, China*

(Received 20 February 2022; revised 13 June 2022; accepted 13 June 2022; published 23 June 2022)

We report the experimental observation of net spin-orbit torques (SOT) in single conductive ferromagnets (FMs), e.g., $\text{Fe}_{20}\text{Ni}_{80}(\text{Py})$, Co, and Ni, despite the system symmetry constraint. Unlike the traditional FM/heavy metal (HM) bilayers, where only the in-plane (IP) damping-like SOT is presented, an unexpected out-of-plane (OOP) damping-like SOT is also unequivocally observed in the single FMs. Using the field angular-dependent, spin-torque ferromagnetic resonance technique, we quantify the IP and OOP SOT efficiencies of 0.018 ± 0.003 and 0.047 ± 0.002 in the pure Py, respectively. We argue that the IP SOT is primarily related to the Py bulk spin Hall effect, while the unconventional SOT is ascribed to the out-of-plane polarized spin current generated from the nonequilibrium spin swapping effect. Additionally, we confirm that such self-induced SOTs also generally exist in the most studied HM/FM multilayer systems, especially for the HMs with low conductivity. Hence, our findings provide a new perspective on understanding SOT control of magnetization reversal and dynamics by an in-plane current in thin, single FM and FM/HM bilayer systems.

DOI: [10.1103/PhysRevB.105.224417](https://doi.org/10.1103/PhysRevB.105.224417)**I. INTRODUCTION**

The interconversion of charge current to spin current is attracting widespread interest in spintronics because the spin current can manipulate the magnetization dynamics with forms of damping-like (DL) torque (τ_{DL}) and field-like (FL) torque (τ_{FL}) [1–4]. Many studies have proved that the spin-orbit torques (SOTs), exerted by the spin current generated from nonmagnetic heavy metal (HM) due to the spin Hall effect (SHE) and/or the interfacial Rashba effect (IRE), can be used to control the magnetization switching and dynamics of the ferromagnet (FM) layer in HM/FM bilayer systems effectively. The spin polarization (torque direction) of the generated spin currents due to SHE and IRE are strictly constrained by the symmetry and crystal structure of these spin polarization materials, e.g., spin current \mathbf{J}_s , spin polarization $\boldsymbol{\sigma}$, and charge current \mathbf{J}_c are mutually orthogonal [5]. Some alternative approaches to generating spin currents with flexible spin polarizations have been theoretically proposed [6] based on the anomalous Hall effect (AHE) [7] and planar Hall effect (PHE) [8] in the conductive ferromagnetic materials, where the magnetization of FMs controls the spin current and its spin polarization directions. Additionally, several experiments find that the spin-orbit coupling (SOC) effect in FMs is nonnegligible, and even the spin Hall angle in some FMs is comparable to heavy metals [9–13]. In such FMs with considerable SHE, the spin polarization of the generated spin currents is independent of the FM magnetization [11,14], in contrast to AHE and PHE mechanisms. Therefore, both the magnetization-dependent and -independent spin current

are expected to be generated in the FMs with SOC due to AHE/PHE and SHE.

As the spin currents with flexible polarization are self-generated in the FMs, a significantly consequent question emerges whether it can induce SOT on itself due to the misalignment between spin polarization and magnetization. Recently, the spin swapping and spin precession effects can generate SOT on themselves in the diffusive ferromagnets, proved in the theoretical aspect [14]. Moreover, several groups experimentally observed a substantial SHE angle by combining spin pumping, inverse SHE, and current-induced SOTs driven magnetization switching [15–17]; and coherent auto-oscillation [18] in the single FM systems. However, the emergence of self-induced SOT in these reports was ascribed to the asymmetry of the studied systems, such as breaking surface/interface [19,20] or crystal (or spatial) symmetry [15,16,21–23]. In contrast, the self-induced DL torque τ_{DL} has also been observed in the single ferromagnetic layer $\text{Co}_{50}\text{Pt}_{50}$ [24] and $\text{Fe}_{0.8}\text{Mn}_{0.2}$ [25] systems without breaking symmetry, which is speculated to be related to the chemical disorder [24] and surface spin rotation [25]. Additionally, it is still elusive that the self-induced τ_{DL} corresponds to the FL effective field for $\text{Fe}_{0.8}\text{Mn}_{0.2}$, while the DL effective field for $\text{Co}_{50}\text{Pt}_{50}$. Although such self-induced SOTs have been reported in the single FM layer and FM/HM bilayer systems, the fundamental mechanisms are still elusive and urgently need further exploration.

This work explores the emergence of the self-induced SOT and its nature in several symmetric FM single-layer and FM/HM bilayer systems. We find that the nonzero self-induced SOT effect is ubiquitous in the single-layer FMs with a strong SOC effect, and contains the conventional DL torque with in-plane (IP) spin polarization and unconventional

^{*}rhliu@nju.edu.cn

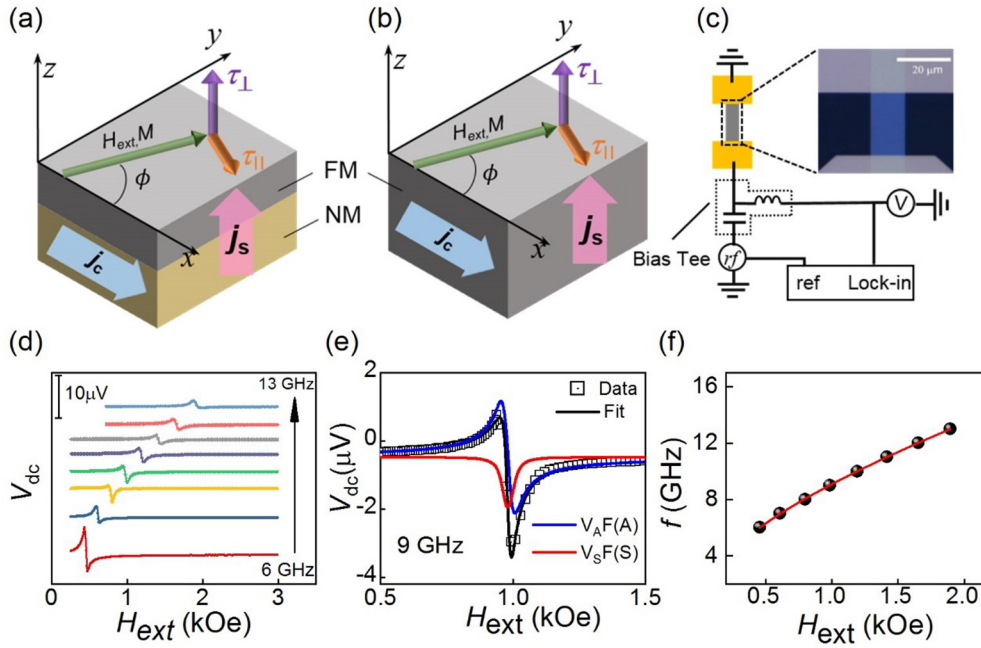


FIG. 1. (a, b) Schematic diagrams illustrating the directions for external magnetic field H_{ext} , applied charge current (j_c), spin current (j_s), and current-induced out-of-plane torque (τ_{\perp}) and in-plane torque (τ_{\parallel}) in NM/FM bilayer (a) and single FM layer (b) systems, respectively. (c) Schematic of the experimental setup and the optical image of the active area of the ST-FMR device. (d) The waterfall plot of ST-FMR spectra of Py(10) obtained at room temperature. (e) The representative ST-FMR spectrum and its fitting curves of Py(10) at 9 GHz. The solid line is the Lorentzian fitting curve, including the symmetric (blue) and antisymmetric (red) parts. (f) Resonance frequency f vs. magnetic field H_{ext} data. Solid line: the Kittel fit.

DL torque with out-of-plane (OOP) spin polarization through angular-dependent, spin-torque ferromagnetic resonance (ST-FMR) and systematic analysis. Combining the bulk SHE and nonequilibrium spin-swapping effects in FMs, we propose a phenomenological model and successfully explain our observed self-induced SOT results.

II. EXPERIMENTAL DETAILS

For SOT systems, a straightforward method to study SOTs is analyzing the SOT-modulated magnetization dynamics. In this work, we adopt the widely recognized ST-FMR technique to study the current-driven magnetization dynamics of single FM metals [21]. In a standard ST-FMR measurement for the FM/HM bilayer system, the HM layer acts as the spin-current source, and the ferromagnetic layer serves as the spin detector, as illustrated in Fig. 1(a). A microwave current (j_c) applied in the HM layer produces spin current (j_s) due to SHE or IRE. Then the spin current vertically flows into the FM layer and exerts both in-plane and out-of-plane SOTs on the magnetic moment of the FM layer. For a single-layer FM system, the FM layer acts as both the spin current source and the spin detector, as Fig. 1(b) shows. Herein, unless otherwise stated, the defined torques configuration and the direction of magnetic field H and current j_c in this work are the same as shown in Fig. 1(a). Figure 1(c) shows the experiment setup and optical image of the test device. In our experiments, the microsize samples were fabricated by combining magnetron sputtering and e-beam lithography, followed by a lift-off process.

III. RESULTS AND DISCUSSION

Our devices consist of the following stacked multi-layers: sapphire substrate/MgO(2 nm)/Fe₂₀Ni₈₀(Py, 10 nm)/MgO(2 nm). Hereafter, we abbreviate the thickness as a single Arabic numeral. Py is first chosen because it is the most popular ferromagnet in spintronics studies. Figure 1(d) shows the ST-FMR spectra of the single-layer Py sample with the excitation frequency ranging from 6 to 13 GHz and an in-plane magnetic field at $\phi = 15^\circ$. The ST-FMR voltage spectrum is fitted using the summation of symmetric and antisymmetric Lorentzian functions:

$$V_{\text{dc}} = V_A \frac{(H_r - H_{\text{ext}})\Delta H}{(H_r - H_{\text{ext}})^2 + \Delta H^2} + V_S \frac{\Delta H^2}{(H_r - H_{\text{ext}})^2 + \Delta H^2}, \quad (1)$$

where ΔH is the linewidth (full width at half maximum of the spectrum), H_r is the resonant magnetic field; and V_A and V_S are the amplitudes of the antisymmetric and symmetric Lorentzian, respectively. Figure 1(e) shows a representative Lorentzian fitting at 9 GHz. After obtaining H_r from Lorentzian fitting, the effective magnetization M_{eff} can be calculated as 9.4 kOe by fitting the frequency-dependent H_r with the Kittel formula, as shown in Fig. 1(f). The M_{eff} is consistent with the uniform Py film [26], indicating the high quality of our samples. From Fig. 1(e), we observe the considerable symmetric Lorentzian component (V_S) that usually corresponds to the conventional SHE-like SOT, indicating the emergence of self-induced SOT in the single-layer Py. It needs to be mentioned that the possible magnonic charge pumping mechanism, previously reported in single-layer Py system [27], may also induce the symmetric Lorentzian sig-

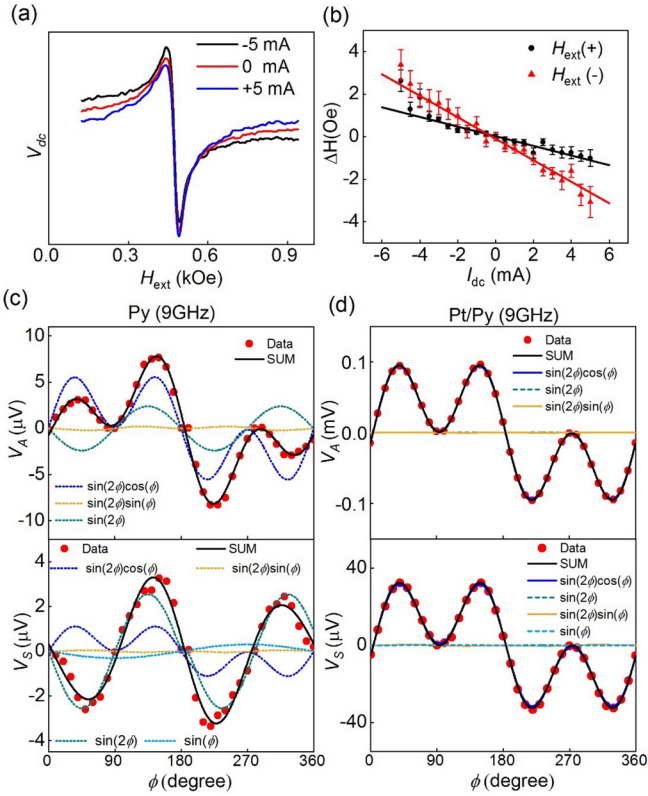


FIG. 2. (a) The representative spectra obtained under three dc currents (-5 , 0 , and $+5$ mA) and the external magnetic field with in-plane angle $\phi = 210^\circ$. (b) Current-induced linewidth changes of Py(10) under positive ($\phi = 30^\circ$) and negative ($\phi = 210^\circ$) magnetic fields. (c) The in-plane, angle-dependent antisymmetric and symmetric components of the ST-FMR spectra for the Py(10) sample. The angular dependence of the antisymmetric parts are fitted by the sum of $\sin(2\phi)\cos(\phi)$, $\sin(2\phi)\sin(\phi)$, and $\sin(2\phi)$; and the symmetric data are fitted by the sum of $\sin(2\phi)\cos(\phi)$, $\sin(2\phi)\sin(\phi)$, $\sin(2\phi)$, and $\sin(\phi)$ functions. (d) Same as (c) for the Pt(6)/Py(6) sample.

nals. However, this presumption can be excluded by the following discussion of the damping modulation experiments. In addition, the fact that the metal ferromagnets with structure or interface asymmetry can generate SOT [20,28] is also eliminated because those asymmetries are absent in our studied system.

To explore the nature of the self-induced SOT, we further adopted a so-called damping modulation scheme in which an additional dc is applied to the device during ST-FMR measurements. Once the charge current induces any SOT on the Py magnetization, the SOT will modify the ST-FMR signal linewidth. Figure 2(a) shows the representative 7-GHz ST-FMR spectra obtained under three dc currents: -5 mA, 0 , and $+5$ mA. The applied dc current can effectively modify both the linewidth and amplitude. Then, we extracted the dc current-dependent linewidth under positive ($\phi = 30^\circ$) and negative ($\phi = 210^\circ$) bias magnetic fields. Figure 2(b) shows an obviously linear modification in linewidth for both bias field directions, consistent with the characteristics of the previous current-induced SOT effects. Since the magnonic charge pumping is insensitive to the dc current, we exclude

the effects of magnonic charge pumping-induced signals in our previous ST-FMR line shape analysis.

From the damping modulation experiment, except for the conclusion of current inducing net SOT in single-layer Py, it is also noted that the linewidth modification slope keeps the same sign with the bias magnetic field reversal. In a typical SHE-dominated system, the current-modulated linewidth usually reverses its sign with magnetization reversal. Thus, the self-induced SOT in the single-layer Py without sign change with magnetization reversal cannot be only attributed to the SHE. We further conducted the in-plane, magnetic field, angle-dependent ST-FMR experiments to make an inside view of the self-induced SOTs. In a SHE-dominated bilayer system, both field angular dependences of V_A and V_S follow the $\sin(2\phi)\cos(\phi)$ symmetry. To verify the reliability of our experimental results and get a direct comparison, we performed similar measurements on the Pt(6)/Py(6) control sample. Figure 2(d) shows that V_A and V_S of the Pt/Py sample follow $\sin(2\phi)\cos(\phi)$ well, consistent with prior results [9,29]. For our single Py sample, both V_A and V_S components show a distinct deviation from the $\sin(2\phi)\cos(\phi)$ dependence, as illustrated in Fig. 2(c). This deviation is qualitatively consistent with the current modulation of the earlier damping experiment. To understand the observed SOT effects more fully, it is necessary to separate the SOT components. As discussed in prior works [6,21,29], the different SOTs exhibit distinct magnetic-field, angle-dependent symmetry. For the general situation, we assume that the self-induced SOT (or the spin current polarization) directions in the Py are arbitrary; thus, field angular dependences of V_A and V_S have the following general formulas [9,30]:

$$V_A \propto \sin(2\phi)(\tau_{x,FL} \sin(\phi) + \tau_{y,FL} \cos(\phi) + \tau_{z,DL}) \quad (2)$$

and

$$V_S \propto \sin(2\phi)(\tau_{x,DL} \sin(\phi) + \tau_{y,DL} \cos(\phi) + \tau_{z,FL}) + \sin(\phi), \quad (3)$$

where the $\tau_{i,j}$ are the torques, with subscripts i (j) indicating the spin current polarization direction (torque types). As for the last term in Eq. (3), spin pumping or heat-related effects may contribute to them [9,20], but the analysis method of angular dependence is still valid. From the fitting results of V_A and V_S in Fig. 2(c), we obtain the nonzero torque terms $\tau_{y,FL}$, $\tau_{z,DL}$, $\tau_{y,DL}$, and $\tau_{z,FL}$. The $\tau_{y,FL}$ and $\tau_{y,DL}$ are the conventional SHE torques produced by the in-plane transverse polarization σ_y spin currents, while the previously unrevealed terms $\tau_{z,DL}$ and $\tau_{z,FL}$ correspond to out-of-plane polarization σ_z spin currents. In other words, the net spin currents with σ_y and σ_z polarizations can be generated in the Py single layer. This anomalous behavior in the linewidth modulation experiments is likely correlated to the self-induced spin currents with σ_z -induced the unconventional SOT effects in Py. For convenience, we preferentially estimate these SOT efficiencies before discussing the origin of the SOT effects.

We define the DL torque efficiencies by dimensionless coefficients, analogous to the spin Hall angle, with the following equations:

$$\xi_{y,\text{DL}} = \frac{\tau_{y,\text{DL}}}{\tau_{y,\text{FL}}} \frac{e\mu_0 M_S t_{\text{Py}}^2}{\hbar} \sqrt{1 + \frac{M_{\text{eff}}}{H_r}} \quad (4)$$

and

$$\xi_{z,\text{DL}} = \frac{\tau_{z,\text{DL}}}{\tau_{y,\text{FL}}} \frac{e\mu_0 M_S t_{\text{Py}}^2}{\hbar} \sqrt{1 + \frac{M_{\text{eff}}}{H_r}}, \quad (5)$$

where e , μ_0 , and \hbar are the electron charge, vacuum permeability, and reduced Planck's constant; and M_S and t_{Py} are the saturation magnetization and the thickness of Py. With taking $M_S = M_{\text{eff}}$ because of a negligible magnetic anisotropy for Py, the $\tau_{y,\text{DL}}$ and $\tau_{z,\text{DL}}$ efficiencies are calculated as $\xi_{y,\text{DL}} = 0.018$ and $\xi_{z,\text{DL}} = 0.047$. The conventional SHE ($\xi_{y,\text{DL}}$) is consistent with the prior spin pumping experimental result [31]. Meanwhile, $\xi_{z,\text{DL}}$ is more than twice the value, ~ 0.019 , of the antiferromagnetic $\text{Mn}_3\text{GaN/Py}$ system [30], indicating that the Py can be a spin current source for the potential application in field-free perpendicular magnetization switching. Using the unconventional spin current generated from Py to switch perpendicular magnetization has been reported in a Py/non-magnetic materials (NM)/FM trilayer device [32,33], whereas the authors considered the out-of-plane SOT from the contribution of the Py/NM interface. Our results of the self-induced SOTs reveal that these magnetic multilayer systems have a more complex SOTs effect than the previous reports. For example, the spin Hall angle varies with different ferromagnets as the spin detector for the same heavy metal in HM/FM. Specifically, the spin Hall angle of Pt was determined as ~ 0.05 with Py as the spin detector [3,34]; the much larger values (>0.10) were determined with Co or CoFeB as the detector [35,36]. The inconsistent spin Hall angle is likely attributed to the different self-induced SOT efficiencies of the ferromagnets themselves. To reaffirm this hypothesis, we further conducted several control experiments and observed the different SOT effects in high-resistance tungsten-based bilayer samples W/Py and W/CoFeB. For convenience, we only analyze the antisymmetric component V_A that reflects the $\xi_{z,\text{DL}}$ information, and its angle dependence is shown in Fig. 3(a) and 3(b). One can see a nonzero component $\tau_{z,\text{DL}}$ in W/Py and W/CoFeB samples. This considerable $\tau_{z,\text{DL}}$ will significantly influence the evaluation of the SOT efficiencies based on line shape analysis. Hence, this is the reason that the spin Hall angle of Pt shows a huge deviation by using different ferromagnets and even different thicknesses as the detector.

In a traditional SOC system, such as the heavy metals Pt, W, and Ta, the SHE-generated spin currents flow along the $\pm z$ -axis with the polarization along the $\pm y$ -axis if the charge current flows along the $\pm x$ -axis. Usually, the spin currents with opposite polarization are equal at each edge or surface. As a result, the net spin currents (or SOT effect) should be canceled entirely in the single symmetric Py system. Before exploring the origin of the observed SOT effects, we first excluded the possible surface/interface origins via systematical interfacial control experiments. Since our single-layer Py sample may have two different interfaces for MgO/Py

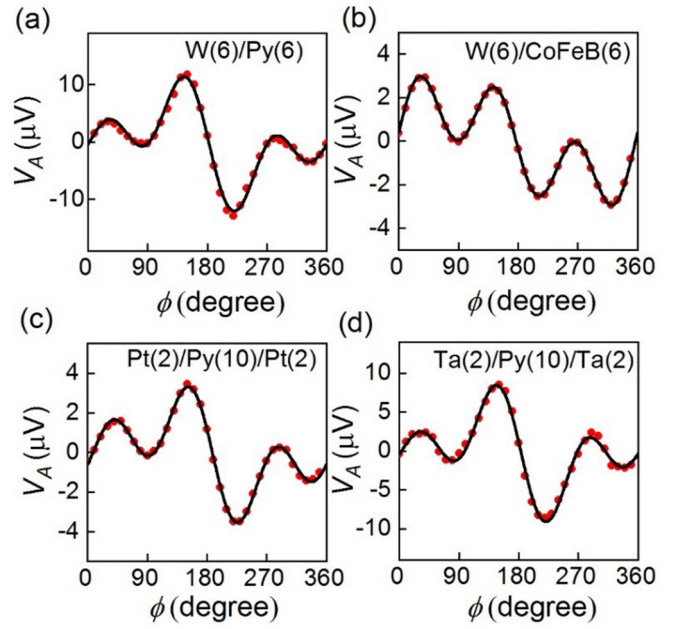


FIG. 3. The angle-dependent V_A components of the ST-FMR spectra of the W(6)/Py(6) sample (a), W(6)/CoFeB(6) sample (b), Pt(2)/Py(10)/Pt(2) sample (c), and Ta(2)/Py(10)/Ta(2) sample (d). The black solid lines are the best fits with the summation of $\sin(2\phi)\cos(\phi)$ and $\sin(2\phi)$ functions.

and Py/MgO, the different interfaces may disturb the analysis because of the different oxidation at such interfaces. To exclude this possibility, we further fabricate two samples with the symmetric structure, e.g., Ta(2)/Py(10)/Ta(2) and Pt(2)/Py(10)/Pt(2), where the asymmetric oxidation of Py can be eliminated. We also focus on the angle dependence of the V_A components, as shown in Fig. 3(c) and 3(d). If the asymmetric interface oxidation generates the SOTs for the MgO/Py/MgO sample, the unconventional torque ($\tau_{z,\text{DL}}$) should be absent in these metal control samples with symmetric structure. However, both the V_A line shape of the Ta(2)/Py(10)/Ta(2) and Pt(2)/Py(10)/Pt(2) samples deviate from the $\sin(2\phi)\cos(\phi)$ symmetry and have an additional $\sin(2\phi)$ term, indicating the existence of $\tau_{z,\text{DL}}$ in these symmetric Py-based control samples. In addition, the V_A line shape of these two control samples is also quite similar and seemingly unrelated to the properties of the capping layer. Thus, we can conclude that the observed SOT effects originate from the bulk effect in Py.

Based on our observation and prior theoretical [14] and experimental results [37,38], we propose a phenomenological scenario involving the spin swapping effect and spin current competing mechanism to explain our observed SOT effect. Because of this competing mechanism, the nominal zero net spin current can still induce the net SOT effect on the FM, and even switch perpendicular magnetization at zero fields through the spin currents with IP polarization [37,38]. The microscopic understanding of the competing mechanism-induced SOT is still elusive. Here, we argue that the spin current competing results in nonequilibrium spin swapping effect probabilities and thus induces a nonzero net OOP SOT effect. In our Py system, the SHE generates equal spin current

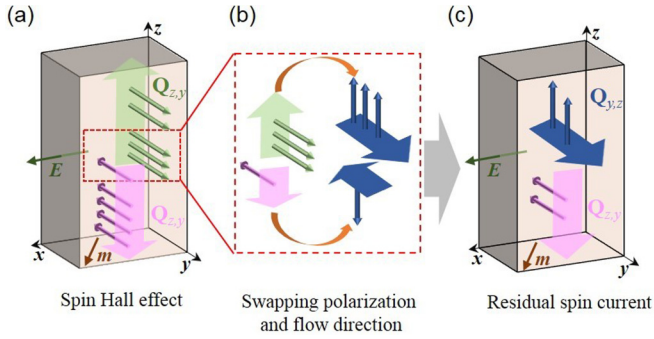


FIG. 4. Schematic diagrams of the generation of the unconventional spin currents in the single FM layer. (a) The spin Hall effect generates two opposite polarized spin currents ($Q_{z,y}$), where the broad arrows indicate the flow direction of spin currents and the small three-dimensional arrows denote the spin polarization. The region, as marked by the dotted red line, represents the spin swapping probabilities of the two opposite spin currents. (b) The schematic of spin swapping process. (c) The residual net spin currents with two spin polarization directions ($Q_{z,y}$ and $Q_{y,z}$) after the spin swapping process.

flows (z -axis) with opposite polarization (y -axis) in the Py, as shown in Fig. 4(a). Then the spin swapping effect changes the spin polarization and the flow direction of the spin currents [39], as illustrated in Fig. 4(b). Due to the nonequilibrium spin swapping probabilities, the residual z -axis polarized and y -axis polarized pure spin currents are nonzero, as shown in Fig. 4(a)–4(c). The nonequilibrium spin swapping probabilities may be related to magnetic moment-dependent scattering in FMs, warranting further studies of the specific intrinsic or extrinsic mechanism, which is beyond the scope of this work. The unconventional SOT effects noted earlier are not restricted to the special FM single layer and should be universal in conductive ferromagnets with SOC effects. To confirm this deduction, we perform the same measurements on other conductive ferromagnets and observe both the conventional and unconventional SOT effects in Ni and Co. The SOT efficiencies ($\xi_{y,DL}$ and $\xi_{z,DL}$) for all studied FMs are summarized in Fig. 5(a). The Ni sample exhibits much higher unconventional ($\xi_{z,DL}$) and SHE-like ($\xi_{y,DL}$) SOT efficiency than the Py and Co single layer. It should be noted that the line shape analysis of the ST-FMR method would overestimate the SOT efficiencies ($\xi_{y,DL}$ and $\xi_{z,DL}$) using Eqs. (4) and (5) because the denominator term $\tau_{y,FL}$ includes not only the I_{RF} -induced Oersted field but also considerable field-like torque here. Furthermore, the previous reports [40,41] found that, contrary to the Co, Fe, and Py systems, the Ni-based multilayer system exhibited the stronger SOC and considerable field-like torque opposite to the Oersted field torque. Therefore, the $\tau_{y,FL}$ is no longer a better term to self-calibrating the I_{RF} by I_{RF} -induced Oersted field torque, consequently causing the huge overestimation of the SOT efficiencies $\xi_{y,DL}$ and $\xi_{z,DL}$ for Ni (or underestimation for Co, Fe, Py) if still using the simple self-calibrated line shape analysis. The additional Ni and Co single-layer results further rule out the possible chemical disorder origination for the self-induced net SOTs for our single-element systems (Ni and Co) [17,24].

Given that the intrinsic unconventional SOT effects are generated in the FMs, such self-generated SOTs are also ex-

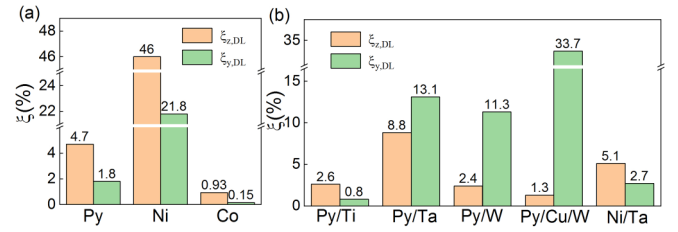


FIG. 5. (a) SHE-like DL SOT efficiency ($\xi_{y,DL}$) and unconventional DL SOT efficiencies ($\xi_{z,DL}$) in single-layer ferromagnetic metals Py(10), Ni(11), and Co(11). (b) The $\xi_{y,DL}$ and $\xi_{z,DL}$ in our studied Py(6)/Ti(6), Py(6)/Ta(6), Py(6)/W(6), Py(6)/Cu(1)/W(6), and Ni(8)/Ta(5) multilayer structure.

pected in the HM/FM multilayer systems because the charge current also flows in the adjacent FM layer in high-resistivity, HMs-based bilayers. Therefore, we fabricated several high-resistivity HM/FM multilayer samples to maximize self-generated SOTs by letting more charge current pass through the Py layer. The obtained SOT efficiencies of these HM/FM samples are summarized in Fig. 5(b). Both the conventional and unconventional SOTs were universally observed. The different unconventional SOT efficiency is related to the variation in resistivity of these heavy metals. Note that the unconventional out-of-plane SOT was not clearly revealed in the prior reports for the Pt/Py bilayer system, which is attributed to the most charge current being shut in the high-conductivity Pt layer rather than the low-conductivity Py layer.

IV. CONCLUSION

In summary, we experimentally demonstrate that the nonzero self-induced SOT effects are universal in the single conductive FM with reserved symmetry and include the conventional SOT with IP transverse polarization and the unconventional SOT with OOP polarization. These self-induced SOTs result from the competing spin swapping and bulk spin Hall effects in the FMs with strong SOC. Our findings support further fundamental understanding of the elusive current-induced SOTs in various hybrid heterostructures with new experimental characteristics.

ACKNOWLEDGMENTS

We acknowledge support from the National Natural Science Foundation of China (Grant No. 12074178) and the Open Research Fund of Jiangsu Provincial Key Laboratory for Nanotechnology.

APPENDIX: DISCUSSION OF HARMONIC HALL MEASUREMENT FOR SINGLE-LAYER PY

To further confirm the observed nontrivial SOT in the single-layer Py, we conduct the independent alternative harmonic Hall voltage measurement. During the measurement, the excitation current is set with amplitude at 2 mA and frequency at 133.3 Hz, and a lock-in amplifier monitors the second harmonic in-plane Hall voltage. The representative in-plane field-dependent harmonic Hall voltage result is shown in Fig. 6. The SOT information in such

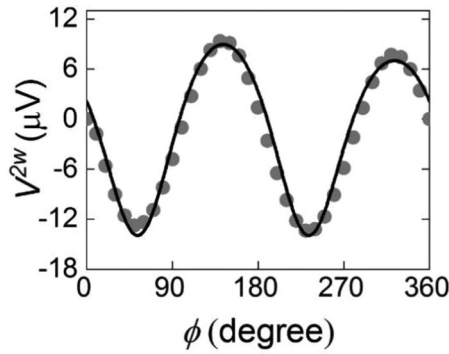


FIG. 6. In-plane field angle (ϕ) dependence of second harmonic Hall voltage for the single-layer Py.

measurement configuration can be analyzed using the field angle-dependent symmetry

$$R^{2\omega} = \frac{R_{\text{PHE}} \cos 2\phi_M}{\gamma(H_{\text{ext}} - H_a \cos 2\phi_M)} (\tau_{y,\text{FL}} \cos 2\phi_M + \tau_{z,\text{DL}}) + R_\phi \cos 2\phi_M, \quad (\text{A1})$$

where R_{PHE} is planar Hall resistance of the sample, R_ϕ is a constant consistent of the contributions of $\tau_{y,\text{DL}}$ and anomalous Nernst effect, $\phi_M = \phi + \frac{H_a \sin 2\phi}{2H_{\text{ext}}} \approx \phi$, because the anisotropic field ($H_a \sim$ several Oersteds) of the Py is much smaller than the applied external field ($H_{\text{ext}} \sim 1000$ Oe). The solid line in Fig. 6 shows the best fit. Based on the fitting, we find the nontrivial spin-orbit torque ($\tau_{z,\text{DL}}$) to SHE-like torque ($\tau_{y,\text{FL}}$) ratio as $\frac{\tau_{z,\text{DL}}}{\tau_{y,\text{FL}}} \sim 20$. The harmonic measurement also shows evidence of the nontrivial spin-orbit torque existence, but it overestimates the nontrivial spin-orbit torque ratio for the Py with a large anisotropy magnetoresistance. The overestimation may be attributed to some artificial origins: (1) since the SHE-like torque-induced effective field is too small in response to a large H_{ext} to be accurately extracted from the angle dependence of the harmonic resistance because the SHE-like SOT efficiency is only 0.018 and (2) since the z -axis spin polarization torque $\tau_{z,\text{DL}}$ does not depend on the in-plane component of magnetization, it can be easily overestimated by a tiny out-of-plane component of magnetization due to an inevitable slight misalignment of the applied magnetic field in experimental measurements.

-
- [1] S. Zhang, P. M. Levy, and A. Fert, Mechanisms of Spin-Polarized Current-Driven Magnetization Switching, *Phys. Rev. Lett.* **88**, 236601 (2002).
- [2] Y. Wang, R. Ramaswamy, and H. Yang, FMR-related phenomena in spintronic devices, *J. Phys. D Appl. Phys.* **51**, 273002 (2018).
- [3] L. Liu, T. Moriyama, D. C. Ralph, and R. A. Buhrman, Spin-Torque Ferromagnetic Resonance Induced by the Spin Hall Effect, *Phys. Rev. Lett.* **106**, 036601 (2011).
- [4] J. C. Slonczewski, Current-driven excitation of magnetic multilayers, *J. Magn. Magn. Mater.* **159**, L1 (1996).
- [5] T. Y. Ma, C. H. Wan, X. Wang, W. L. Yang, C. Y. Guo, C. Fang, M. K. Zhao, J. Dong, Y. Zhang, and X. F. Han, Evidence of magnetization switching by anomalous spin Hall torque in NiFe, *Phys. Rev. B* **101**, 134417 (2020).
- [6] C. Ciccarelli, L. Anderson, V. Tshitoyan, A. J. Ferguson, F. Gerhard, C. Gould, L. W. Molenkamp, J. Gayles, J. Železný, L. Šmejkal, Z. Yuan, J. Sinova, F. Freimuth, and T. Jungwirth, Room-temperature spin-orbit torque in NiMnSb, *Nat. Phys.* **12**, 855 (2016).
- [7] T. Taniguchi, J. Grollier, and M. D. Stiles, Spin-Transfer Torques Generated by the Anomalous Hall Effect and Anisotropic Magnetoresistance, *Phys. Rev. Appl.* **3**, 044001 (2015).
- [8] C. Safranski, J. Z. Sun, J.-W. Xu, and A. D. Kent, Planar Hall Driven Torque in a Ferromagnet/Nonmagnet/Ferromagnet System, *Phys. Rev. Lett.* **124**, 197204 (2020).
- [9] W. L. Yang, J.W. Wei, C. H. Wan, Y.W. Xing, Z. R. Yan, X. Wang, C. Fang, C. Y. Guo, G. Q. Yu, and X. F. Han, Determining spin-torque efficiency in ferromagnetic metals via spin-torque ferromagnetic resonance, *Phys. Rev. B* **101**, 064412 (2020).
- [10] B. F. Miao, S. Y. Huang, D. Qu, and C. L. Chien, Inverse Spin Hall Effect in a Ferromagnetic Metal, *Phys. Rev. Lett.* **111**, 066602 (2013).
- [11] V. P. Amin, J. Li, M. D. Stiles, and P. M. Haney, Intrinsic spin currents in ferromagnets, *Phys. Rev. B* **99**, 220405(R) (2019).
- [12] G. Qu, K. Nakamura, and M. Hayashi, Magnetization direction dependent spin Hall effect in 3D ferromagnets, *Phys. Rev. B* **102**, 144440 (2020).
- [13] J. A. Mittelstaedt and D. C. Ralph, Resonant Measurement of Nonreorientable Spin-Orbit Torque from a Ferromagnetic Source Layer Accounting for Dynamic Spin Pumping, *Phys. Rev. Appl.* **16**, 024035 (2021).
- [14] C. O. Pauyac, M. Chshiev, A. Manchon, and S. A. Nikolaev, Spin Hall and Spin Swapping Torques in Diffusive Ferromagnets, *Phys. Rev. Lett.* **120**, 176802 (2018).
- [15] M. Tang, K. Shen, S. Xu, H. Yang, S. Hu, W. Lü, C. Li, M. Li, Z. Yuan, S. J. Pennycook, K. Xia, A. Manchon, S. Zhou, and X. Qiu, Bulk spin torque-driven perpendicular magnetization switching in L10 FePt single layer, *Adv. Mater.* **32**, 2002607 (2020).
- [16] Z. Zheng, Y. Zhang, V. Lopez-Dominguez, L. Sánchez-Tejerina, J. Shi, X. Feng, L. Chen, Z. Wang, Z. Zhang, K. Zhang, B. Hong, Y. Xu, Y. Zhang, M. Carpentieri, A. Fert, and G. Finocchio, W. Zhao, and P. K. Amiri, Field-free spin-orbit torque-induced switching of perpendicular magnetization in a ferrimagnetic layer with a vertical composition gradient, *Nat. Commun.* **12**, 4555 (2021).
- [17] Z. Chen, L. Liu, Z. Ye, Z. Chen, H. Zheng, W. Jia, Q. Zeng, N. Wang, B. Xiang, T. Lin, J. Liu, M. Qiu, S. Li, J. Shi, P. Han, and H. An, Current-induced magnetization switching in a chemically disordered A1 CoPt single layer, *Appl. Phys. Express* **14**, 033002 (2021).

- [18] M. Haidar, A. A. Awad, M. Dvornik, R. Khymyn, A. Houshang, and J. Åkerman, A single layer spin-orbit torque nanoscillator, *Nat. Commun.* **10**, 2362 (2019).
- [19] W. Wang, T. Wang, V. P. Amin, Y. Wang, A. Radhakrishnan, A. Davidson, S. R. Allen, T. J. Silva, H. Ohldag, D. Balzar, B. L. Zink, P. M. Haney, J. Q. Xiao, D. G. Cahill, V. O. Lorenz, and X. Fan, Anomalous spin-orbit torques in magnetic single-layer films, *Nat. Nanotechnol.* **14**, 819 (2019).
- [20] T. Seki, Y.- C. Lau, S. Iihama, and K. Takanashi, Spin-orbit torque in a Ni-Fe single layer, *Phys. Rev. B* **104**, 094430 (2021).
- [21] D. Fang, H. Kurebayashi, J. Wunderlich, K. Výborný, L. P. Zârbo, R. P. Campion, A. Casiraghi, B. L. Gallagher, T. Jungwirth, and A. J. Ferguson, Spin-orbit-driven ferromagnetic resonance, *Nat. Nanotechnol.* **6**, 413 (2011).
- [22] X. Xie, X. Zhao, Y. Dong, X. Qu, K. Zheng, X. Han, X. Han, Y. Fan, L. Bai, Y. Chen, Y. Dai, Y. Tian, and S. Yan, Controllable field-free switching of perpendicular magnetization through bulk spin-orbit torque in symmetry-broken ferromagnetic films, *Nat. Commun.* **12**, 2473 (2021).
- [23] L. Zhu, D. C. Ralph, and R. A. Buhrman, Unveiling the mechanism of bulk spin-orbit torques within chemically disordered FexPt1-x single layers, *Adv. Funct. Mater.* **31**, 2103898 (2021).
- [24] L. Zhu, X. S. Zhang, D. A. Muller, D. C. Ralph, and R. A. Buhrman, Observation of strong bulk damping-like spin-orbit torque in chemically disordered ferromagnetic single layers, *Adv. Funct. Mater.* **30**, 2005201 (2020).
- [25] Z. Luo, Q. Zhang, Y. Xu, Y. Yang, X. Zhang, and Y. Wu, Spin-Orbit Torque in a Single Ferromagnetic Layer Induced by Surface Spin Rotation, *Phys. Rev. Appl.* **11**, 064021 (2019).
- [26] Y. Huo, C. Zhou, L. Sun, S. T. Chui, and Y. Z. Wu, Multiple low-energy excitation states in FeNi disks observed by broadband ferromagnetic resonance measurement, *Phys. Rev. B* **94**, 184421 (2016).
- [27] A. Azevedo, R. O. Cunha, F. Estrada, O. Alves Santos, J. B. S. Mendes, L. H. Vilela-Leão, R. L. Rodríguez-Suárez, and S. M. Rezende, Electrical detection of ferromagnetic resonance in single layers of permalloy: Evidence of magnonic charge pumping, *Phys. Rev. B* **92**, 024402 (2015).
- [28] M. Aoki, E. Shigematsu, R. Ohshima, T. Shinjo, M. Shiraishi, and Y. Ando, Current-induced out-of-plane torques in a single permalloy layer with lateral structural asymmetry, *Phys. Rev. B* **105**, 144407 (2022).
- [29] D. MacNeill, G. M. Stiehl, M. H. D. Guimaraes, R. A. Buhrman, J. Park, and D. C. Ralph, Control of spin-orbit torques through crystal symmetry in WTe₂/ferromagnet bilayers, *Nat. Phys.* **13**, 300 (2016).
- [30] T. Nan *et al.*, Controlling spin current polarization through non-collinear antiferromagnetism, *Nat. Commun.* **11**, 4671 (2020).
- [31] H. Wang, C. Du, P. C. Hammel, and F. Yang, Spin current and inverse spin Hall effect in ferromagnetic metals probed by Y₃Fe₅O-based spin pumping, *Appl. Phys. Lett.* **104**, 202405 (2014).
- [32] S.- H. C. Baek, V. P. Amin, Y.- W. Oh, G. Go, S.- J. Lee, G.- H. Lee, K.- J. Kim, M. D. Stiles, B.- G. Park, and K.- J. Lee, Spin currents and spin-orbit torques in ferromagnetic trilayers, *Nat. Mater.* **17**, 509 (2018).
- [33] Y.- W. Oh, J. Ryu, J. Kang, and B.-G. Park, Material and thickness investigation in Ferromagnet/Ta/CoFeB trilayers for enhancement of spin-orbit torque and field-free switching, *Adv. Electron. Mater.* **5**, 1900598 (2019).
- [34] Y. Wang, P. Deorani, X. Qiu, J. H. Kwon, and H. Yang, Determination of intrinsic spin Hall angle in Pt, *Appl. Phys. Lett.* **105**, 152412 (2014).
- [35] W. Zhang, W. Han, X. Jiang, S.-H. Yang, and S. S. P. Parkin, Role of transparency of platinum-ferromagnet interfaces in determining the intrinsic magnitude of the spin Hall effect, *Nat. Phys.* **11**, 496 (2015).
- [36] M.- H. Nguyen, C.- F. Pai, K. X. Nguyen, D. A. Muller, D. C. Ralph, and R. A. Buhrman, Enhancement of the anti-damping spin-torque efficacy of platinum by interface modification, *Appl. Phys. Lett.* **106**, 222402 (2015).
- [37] Q. Ma, Y. Li, D. B. Gopman, Y. P. Kabanov, R. D. Shull, and C. L. Chien, Switching a Perpendicular Ferromagnetic Layer by Competing Spin Currents, *Phys. Rev. Lett.* **120**, 117703 (2018).
- [38] Z. A. Bekele, X. Liu, Y. Cao, and K. Wang, High-efficiency spin-orbit torque switching using a single heavy-metal alloy with opposite spin Hall angles, *Adv. Electron. Mater.* **7**, 2000793 (2021).
- [39] M. B. Lifshits and M. I. Dyakonov, Swapping Spin Currents: Interchanging Spin and Flow Directions, *Phys. Rev. Lett.* **103**, 186601 (2009).
- [40] C. Du, H. Wang, F. Yang, and P. C. Hammel, Systematic variation of spin-orbit coupling with *d*-orbital filling: Large inverse spin Hall effect in 3D transition metals, *Phys. Rev. B* **90**, 140407(R) (2014).
- [41] A. Bose, H. Singh, V. K. Kushwaha, S. Bhuktare, S. Dutta, and A. A. Tulapurkar, Sign Reversal of Fieldlike Spin-Orbit Torque in an Ultrathin Cr/Ni Bilayer, *Phys. Rev. Appl.* **9**, 014022 (2018).